

Improved CO₂ capture performance of electrochemically mediated amine regeneration processes with ionic surfactant additives

Mohammad Rahimi¹, Federico Zucchelli^{1,2}, Monica Puccini², T. Alan Hatton^{1,*}

¹ Department of Chemical Engineering, Massachusetts Institute of Technology, Cambridge, MA 02139, USA

² Department of Civil and Industrial Engineering, University of Pisa, Largo Lucio Lazzarino 2, 561226 Pisa, Italy

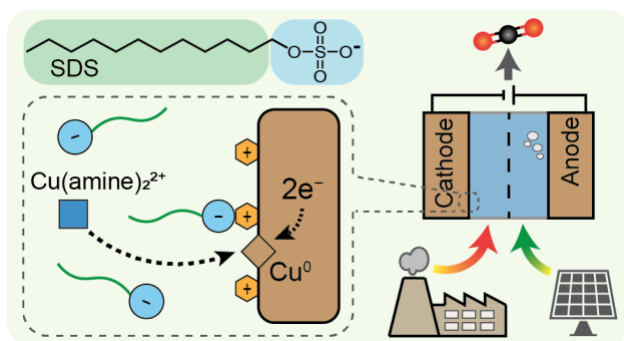
* Corresponding author: tahatton@mit.edu

Abstract

For the effective reduction of global CO₂ emissions, it is essential to develop and deploy efficient and cost-effective technologies for CO₂ capture, especially from large point sources. We recently developed an electrochemically mediated amine regeneration (EMAR) system to replace traditional thermal desorption for the capture of CO₂ from post-combustion flue gases. Despite EMAR effectiveness on a laboratory scale, concerns regarding the high gas-to-liquid ratio in the electrochemical cell and long-term instability of the electrodes need to be addressed before further scale-up of the process to a pilot plant and beyond can be entertained. Accordingly, we investigated the effect of using sodium dodecyl sulfate (SDS) as an anionic surfactant and dodecyltrimethylammonium bromide (DTAB) as a cationic surfactant on the process operation. It was found that it is advantageous to use an anionic surfactant for a system such as EMAR that contains hydrophilic electrodes and a positively charged electrochemically active species. The overall cell resistance was notably reduced when SDS anionic surfactant was used. The precipitation of copper particles observed in the anode outlet when no surfactant was used was effectively avoided when SDS was added to the electrolyte, resulting in electrode stability. In addition, smaller gas bubbles were produced in the presence of the SDS surfactant, which resulted in less blockage of the electrode by the gas with a resultant lower cell potential under constant current conditions, driving more efficient CO₂ desorption. This led to an approximate 25% reduction in the electrochemical energy requirement, the lowest ever achieved experimentally for the EMAR process. Overall, the addition of a very low concentration of SDS resulted in the successful circumvention of the important problems faced by the EMAR system regarding further scale-up.

Keywords: CO₂ capture, electrochemical process, surfactant, SDS, DTAB, energetics

TOC



Introduction

The anthropogenic release of greenhouse gases, especially carbon dioxide (CO₂), has been cited repeatedly^{1, 2} as the most significant contribution to the observed increase in average global temperature since the mid-20th century. To ensure a margin of no more than 1.5°C global temperature increase by the end of the century, it is crucial that interim technologies such as carbon capture and storage (CCS) are deployed, especially for large point sources, to effectively reduce global CO₂ emissions.³ State-of-the-art technology for carbon capture (also known as CO₂ separation) from large point sources such as industrial flue gases utilizes the amine scrubbing process with thermally driven amine regeneration.⁴ Despite their technological maturity, amine-based thermal scrubbing processes face several challenges that have hindered their deployment, including high regeneration energy penalty, degradation of amines at high temperatures, and high operational costs.^{5, 6} Efforts to address the challenges faced by thermal scrubbing processes remain ongoing.

A fundamentally different approach has recently garnered attention, one that employs electrochemical rather than thermal processes to drive CO₂ desorption and absorbent regeneration. Renewable sources of energy can be exploited to compensate for the energy penalty of such processes, offering an attractive route for CO₂ capture with a minimal carbon footprint. Several new electrochemical approaches have been introduced and developed over just the last few years; this branch of CCS is rapidly emerging. In this context, electrochemical cycles have been employed to generate nucleophiles,⁷⁻⁹ modulate solution

pH,¹⁰⁻¹² exploit capacitive swing behavior,¹³⁻¹⁵ and engage metal-carbon batteries,^{16, 17} to enable selective separation of CO₂ from various sources, including flue gas and air.

Recently, an electrochemically mediated amine regeneration (EMAR) system was developed as an alternative method to the conventional thermal regeneration of amines with the goal of reducing the energy demand of the CO₂ capture process and minimizing amine degradation by operating the process at a low temperature.^{18, 19} The process relies on the competitive binding between CO₂ and a suitable metallic ion (e.g., Cu²⁺) to an absorbent amine molecule, e.g., ethylenediamine (EDA). Similar to thermal approaches, CO₂ is absorbed by the amine in an absorption column. However, instead of a thermal swing to regenerate the amine, the CO₂-rich amine stream from the absorber is introduced to the anode compartment of an electrochemical cell, where copper ions are generated electrochemically from a copper plate anode (i.e., Cu⁰ → Cu²⁺ + 2e⁻) to drive the dissociation of amine-CO₂ to release CO₂ (i.e., Cu²⁺ + 2 EDA-CO₂ → Cu(EDA)₂²⁺ + 2 CO₂). The gas is subsequently separated through a flash tank located after the anode compartment. The CO₂-lean (Cu-rich) stream is then regenerated via the electrochemical plating of copper on the cathode from the copper-amine complex (i.e., Cu(EDA)₂²⁺ + 2e⁻ → Cu⁰ + 2 EDA). The regenerated amines are sent to the absorption column for further CO₂ capture (Figure 1). Thus, CO₂ separation can be achieved by chemical absorption followed by electrochemical desorption and regeneration of the absorbent through the EMAR process.

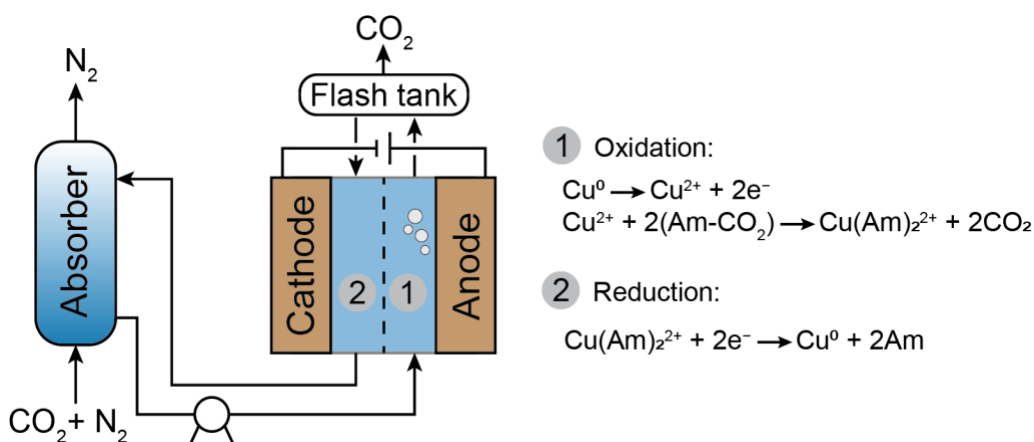


Figure 1. A schematic of the EMAR process with copper electrodes and an amine (noted as “Am”) as the absorbent.

In recent years, the EMAR process has been advanced on many fronts. A laboratory-scale plant was constructed and scaled up to a level at which continuous CO₂ capture from simulated flue gas was achieved over 100 hours of operation, spanning 50 absorption/desorption cycles.²⁰ A techno-economic analysis of this process found it to be competitive with the state-of-the-art thermal amine approaches in terms of energy requirement and associated capture costs.²¹ However, some concerns relating to the long-term operation of the EMAR process remain, which must be addressed prior to its actual implementation for CO₂ capture. The experimental flow-mode demonstration of the process showed a large volumetric CO₂ desorption rate, significantly higher (5–7 times) than that of the liquid flow. The high flow rate of the gas desorbed within the anode compartment may result in washing out of the metastable copper layer on the electrode surface that is subjected to gradual oxidation (proportional to the electrical current). This potentially leads to electrode instability, resulting in loss of the electrode during long-term operation. In our previous experiments, a notable quantity of copper precipitate was observed leaving the anode compartment after the cell was run for a few hours, which highlights the electrode instability issue originating from the high gas flow rate. In addition, ideally, the electrode surface should be covered only by liquid since electrochemically active species (e.g., Cu(EDA)₂²⁺) are dissolved in the aqueous phase. When a portion of the electrode is exposed to the gas phase, however, there is a lower available surface area for electrochemical reactions, resulting in a higher energy requirement for the process.

The unfavorable impacts of the high gas flow rate can be minimized by using conventional surfactants. The utilization of a surfactant in the EMAR electrolyte could be beneficial in two ways: achieving a controlled plating/stripping process^{22, 23} and producing smaller bubbles^{24, 25}. A high-quality copper deposition layer that is formed on the cathode in the presence of a surfactant undergoes controlled smooth stripping when the electrode functions as the anode following the switch in polarity, making it more resistant to physical instability. Moreover, a desorbed gas stream containing smaller bubbles can be obtained as a result of the reduction in electrolyte surface tension when using a surfactant which could be substantially beneficial in terms of the overpotential required for the process.

In the present study, the effect on EMAR performance of two ionic surfactants was investigated: sodium dodecyl sulfate (SDS) as an anionic and dodecyltrimethylammonium bromide (DTAB) as a cationic amphiphile. Our preliminary results indicated that for EMAR,

as an electrochemical process, the ionic surfactants perform better than nonionic surfactants (e.g., Triton X-100; see Figure S1 in the Supporting Information). In addition, these ionic surfactants are inexpensive, environmentally benign compounds widely used in a variety of applications, including as effective additives in electrochemical systems.^{26, 27} As ionic surfactants, these compounds consist of a charged hydrophilic head group attached to a hydrophobic tail. The influence of these additives on various aspects of the EMAR process was investigated in detail, including their effects on the CO₂ absorption rate and capacity, electrochemical performance, gas desorption rate, electrode stability, and energy requirement. An EMAR cycle with copper electrodes and an equimolar solution of EDA and aminoethylethanolamine (AEEA) as the absorbent was used, which has previously been confirmed as the optimized chemistry to run the system.²⁰

Materials and Methods

Absorption rate and CO₂ loading measurements. To evaluate the absorption rate and CO₂ loading, 15 mL electrolyte containing 0.25 mol/kg (molal, noted as “m”) CuSO₄, 0.5 m EDA and 0.5 m AEEA amines, 0.5 m Na₂SO₄ supporting electrolyte, and an additional 1 millimolal (noted as “mm”) SDS or DTAB was purged with a constant pure CO₂ flow for 25 minutes to ensure complete saturation of the electrolyte. The CuSO₄ concentration used in absorption tests was the average value of the anolyte (0.1 m) and catholyte (0.4 m) concentrations of the EMAR cycle. The pH of the solution was measured (using a pH probe; Orion™ PerpHecT™ ROSS™) to compare the absorption rates of different electrolytes, since changes in pH values could be effectively translated into amounts of CO₂ absorbed. The CO₂ loading, defined as the moles of CO₂ absorbed per mole of amine, was estimated by measuring the volume of gaseous CO₂ released upon acidification of the sample. Further details regarding the solution preparation and CO₂ loading measurement can be found in the Supporting Information.

Electrochemical analysis. The electrochemical reaction under various electrolyte conditions was analyzed using cyclic voltammetry (CV), which was performed in a standard three-electrode cell with an Ag/AgCl (+0.211 V vs. SHE; RE-5B; BASi) reference electrode, a glassy carbon working electrode, and a platinum wire as a counter electrode. CV was run

over a potential range of -0.8 to 0.5 V, with a scan rate of 50 mV/s. Electrochemical impedance spectroscopy (EIS) was used to quantitate different components of electrochemical resistance, including ohmic (solution and membrane), charge transfer, and diffusion resistances. All EIS experiments were measured under a whole cell offset of 0.2 V over a frequency range of 100 kHz to 0.1 Hz, with a sinusoidal amplitude of 10 mV, as previously described.^{28, 29} The EIS data were fit to a Randles circuit model to identify the different components of the resistance.

Electrochemical cell configuration and operation. The electrochemical performance of the EMAR process with additional surfactant in the electrolyte was evaluated in a two-compartment cell that we previously developed.¹⁹ In brief, the cell consists of two copper plate electrodes (23 cm \times 10 cm each) separated by two flow channels and a membrane (Selemion AMV, Asashi Glass, Japan) to prevent convective mixing of the anolyte and catholyte streams. A heating jacket operated with water as the fluid was devised to allow direct heating of the electrode in order to maintain isothermal operation at 50°C . Several gaskets were used to seal the flow channels, and the cell was secured by two compression plates held on either side of the unit (Figure 2). A power supply (9122A B&K Precision, USA) was used to drive current through the cell, and the cell potential was recorded during the experiment.

The electrolytes containing mixed amines with various concentrations of SDS surfactant were saturated with the desired gas composition in advance. The anolyte contained 0.1 m CuSO_4 and was saturated with 15% CO_2 (85% N_2) at a solution temperature of 50°C , which is the simulated flue gas temperature at the bottom of the absorber. The catholyte contained 0.4 m CuSO_4 and was saturated with 100% CO_2 at 50°C . The electrolytes were transferred to the chambers using peristaltic pumps (OEM Reglo, Cole-Parmer, USA) at a flowrate of 1 mL/min, a value chosen based on the cell volume to achieve desirable copper ion concentration shifts along the cell (anolyte: 0.1 – 0.4 m; catholyte: 0.4 – 0.1 m).³⁰ The two-phase gas–liquid stream leaving the anode compartment was sent to a glass bottle (i.e., flash tank) to disengage CO_2 desorbed during the process. The gas leaving the flash tank passed through a condenser prior to being analyzed by a mass flow meter (MFM; Aalborg, USA) and an infrared (IR) sensor (Figure 2). The energy requirement of the electrochemical process was estimated by considering the CO_2 desorption rate and cell potential as described previously.¹⁹

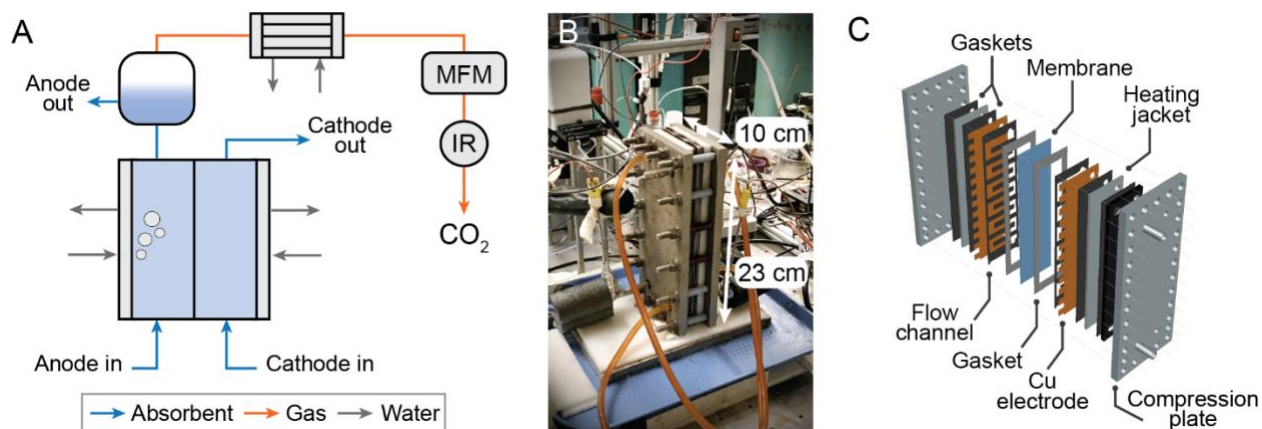


Figure 2. (A) A process flow diagram of the EMAR process with a two-compartment electrochemical cell to investigate the effect of the presence of surfactant in the electrolyte. The gas desorbed from the anode chamber is sent to the flash tank equipped with a condenser for gas-liquid separation, and subsequently passed through a mass flow meter (MFM) and an infrared (IR) sensor to measure the flow rate and CO₂ fraction of the stream, respectively. (B) The photo and (C) the exploded view show the electrochemical cell used for the experiments, in which the copper electrodes, flow channels, gaskets, membrane, and compression plates are sandwiched together.

Results and Discussion

Comparison of anionic and cationic surfactants. The effects of using SDS as an anionic surfactant and DTAB as a cationic surfactant on the CO₂ absorption rates and basic electrochemical properties of the EMAR system were investigated. To evaluate the absorption rates, electrolytes of different composition were purged with pure CO₂ and the solution pH was recorded. The results show that the pH profiles were not affected by the addition of either SDS or DTAB surfactants, indicating that these additional compounds do not interfere with the amine absorption mechanism (Figure 3A). This is especially important for operation of the cell on a large scale, since the absorption column previously developed for the EMAR process can still be employed in the presence of surfactants, with no required modification in terms of size or configuration, avoiding additional capital costs. The only concern associated with the use of surfactants in the absorption column would be foaming, which can be easily handled using very low concentrations of a cost-effective anti-foaming agent (also known as defoamer) such as polydimethylsiloxane.^{31, 32} For the investigated concentrations of the surfactants (1 mM), no significant foaming was observed. In addition, the total CO₂ capacity of the solution was not affected by the surfactants, as indicated by

achievement of the same CO₂ loadings with and without surfactant present (Figure 3A inset). This confirms that neither anionic (SDS) nor cationic (DTAB) surfactants react with the EDA and AEEA amine species; hence, the amines are effectively available to capture CO₂. Overall, electrolytes containing either SDS or DTAB surfactant perform as well as the original EMAR solution in terms of the absorption kinetics and capacity.

Cyclic voltammetry (CV) was employed to investigate the electrochemical activities of the EMAR electrolytes with or without the surfactants. The results indicate a marked difference between the anionic and cationic surfactants, since both the reduction and oxidation peaks were highly dependent on the type of surfactant used (Figure 3B). The addition of a very low quantity of the SDS anionic surfactant (1 mM, which is 250-fold lower than Cu(amine)₂²⁺ as the electrochemically active species) resulted in notable improvements in the obtained peaks, confirming that the stripping/plating reactions of copper were facilitated in the presence of this surfactant. In contrast, addition of the same amount of the DTAB cationic surfactant resulted in a reduction in the electrochemical performance, since both the oxidation and reduction peaks were suppressed as compared with those of the original EMAR electrolyte with no surfactant (noted as “NS”). CV results performed at a different scan rate showed the same performance trend (i.e., the highest for SDS and the lowest for DTAB; see Figure S2 in the Supporting Information). In addition, a solution containing only the surfactants and no copper ions or amines exhibited no peaks in the CV measurements, indicating electrochemical inactivity of the surfactant itself, which is essential, otherwise it would result in parasitic electrochemical reactions that lower the overall Faradaic efficiency of the desorption process as well as degradation of the surfactants.

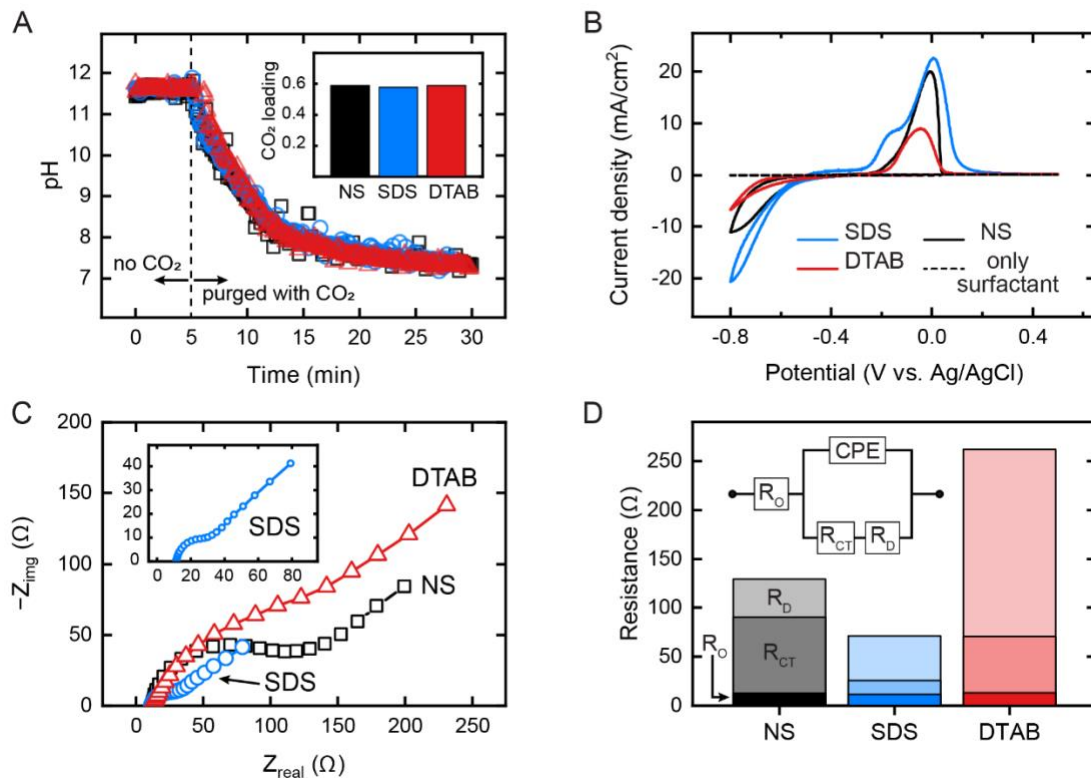


Figure 3. Comparison of (A) absorption rates under saturation with CO₂ for 25 min and the final CO₂ loading (inset); (B) CV conducted over a potential range of -0.8 to 0.5 V (vs. Ag/AgCl) at a scan rate of 5 mV/s; (C) Nyquist plot representative of the EIS experiment; and (D) an indication of the components of the cell resistance of the EMAR electrolyte containing 0.25 m CuSO₄, 0.5 m Na₂SO₄ supporting electrolyte, 0.5 m EDA, and 0.5 m AEEA with either no surfactant (NS), 1 mM SDS, or 1 mM DTAB. The EIS data were fit to a Randles circuit model (inset in panel D) to identify the different components of resistance, including ohmic (R_o), charge transfer (R_{CT}), and diffusion (R_D ; reported for a frequency value of 1 Hz) resistances and a constant phase element (CPE). The fitting errors were less than 5% .

Electrochemical impedance spectroscopy (EIS) was used to quantitate the components of electrochemical resistance with a view to investigating the impact of using either anionic or cationic surfactants. In all scenarios, a semi-circle followed by a tail was observed in the Nyquist plot, which is characteristic of a system with a Randles-equivalent circuit (Figure 3C). The results show that the charge transfer and diffusion components of the resistance were highly impacted by the type of surfactant (Figure 3D); however, the addition of surfactant did not affect the ohmic resistance, which consists of solution and membrane resistances (Figure S3). This indicates that surfactants with relatively large molecular sizes do not block the membrane exchange sites, which would negatively impact the (electro)migration of species. The charge transfer resistance varied substantially depending

on the type of surfactant used. The use of SDS anionic surfactant resulted in more than an 80% reduction in charge transfer resistance as compared with that in the absence of surfactant; this reduction was less significant (~25%) in the presence of DTAB cationic surfactant. The diffusion resistance, which is resistance toward diffusion of the electrochemically active species through the diffusion layer to reach the electrode, of the investigated electrolytes was different. In general, addition of the surfactant increased the diffusion resistance. In the case of SDS, a slight increase of only 15% was observed, while this increase was significant following addition of DTAB to the electrolyte (~400% increase as compared with that in the absence of surfactant). Considering all the components of resistance, the lowest value was obtained for electrolyte containing SDS surfactant. The constant phase element (CPE) was modeled as an ideal capacitor. The obtained CPE values (0.6 mF for no surfactant; 0.4 mF for SDS; 0.1 mF for DTAB) indicated that using surfactants result in lowering the capacitance. This could be due to the formed layer of surfactant which likely resulted in reducing the dielectric constant, and hence, the capacitance.

The CV and EIS findings highlight the crucial role of surfactant type on performance. To explain this, the ionic surfactant adsorption orientation on a hydrophilic surface (such as the Cu electrode) and the resulting interaction with the electrochemically active species should be carefully considered. As repeatedly reported,³³⁻³⁵ ionic surfactants tend to adsorb by their charged head rather than their hydrophobic tail onto a hydrophilic electrode. In terms of layer configuration, if the charge of the surfactant head group is opposite that of the electrode charge, bilayer adsorption occurs on the electrode,^{36, 37} which could be due to the additional electrostatic forces making the first adsorbed layer relatively stable. If the charge of the surfactant head group is the same as the electrode charge, despite the electrostatic repulsion, minor adsorption of the surfactant on the electrode is still observed experimentally.³⁸⁻⁴⁰ In the case of EMAR with high concentrations of the supporting electrolyte salt, surfactants with the same charge as the electrode are likely adsorbed on a layer of ions with an opposite charge formed on the electrode, e.g., Na⁺ on the cathode, that screens the surfactant/electrode charge interactions (Figure 4).

The specific structure of the adsorbed surfactant layer on the electrode is likely responsible for the significant differences in resistance observed following the addition of SDS or DTAB to the EMAR electrolyte. Here, we discuss the cathode electrode and its reactions, since it is the main limiting electrochemical reaction in the EMAR cycle. It has been shown

that surfactants have an electrocatalytic effect that results in a reduction of the energy barrier for nucleation,⁴¹ which is a necessary step for copper deposition. The lower charge transfer resistances observed in the presence of a surfactant can be attributed to this catalytic effect. The charge transfer resistance of the solution was impacted less by DTAB than that by SDS. On the negatively charged cathode, the surface electric field is reduced in the presence of adsorbed DTAB as a result of local charge neutralization,^{37, 42} which potentially causes an increase in the charge transfer resistance; the electrocatalytic effect to reduce the charge transfer is offset significantly by the local charge neutralization effect. These observations can be used to interpret the differences in charge transfer resistance between the samples observed in the EIS measurements (Figure 3D).

In addition to the impact on the charge transfer resistance, the addition of the surfactant can affect the diffusion resistance. Focusing on the cathode, we note that the electrochemically active species (i.e., $\text{Cu}(\text{amine})_2^{2+}$) must pass through the diffusion layer to reach the electrode surface prior to the exchange of electrons with the electrode (which accounts for charge transfer resistance, as discussed). In the presence of SDS, the diffusion of the positively charged electroactive species through the weakly adsorbed layer of the surfactant results in an additional diffusion resistance as compared with that in the absence of surfactant. In the case of DTAB, the more strongly adsorbed surfactant bilayer provides a significantly greater resistance to the diffusion of the charged species to the electrode surface than does the SDS layer. In addition, the outer layer of the bilayer is positively charged (as a result of DTAB cationic head groups) (Figure 4), which further repels $\text{Cu}(\text{amine})_2^{2+}$ species, contributing to the significant diffusion resistance, as observed in the EIS measurement (Figure 3D). Overall, the beneficial impact of the reduced charge transfer resistance in the case of an anionic surfactant such as SDS as well as the detrimental effect of the additional diffusion resistance in the presence of a cationic surfactant such as DTAB explains the electrochemical performance measured in the CV experiments (highest for SDS, followed by no surfactant and DTAB). Therefore, for a system such as EMAR with hydrophilic electrodes and a positively charged electroactive species, it is essential to use an anionic surfactant to improve the electrochemical performance.

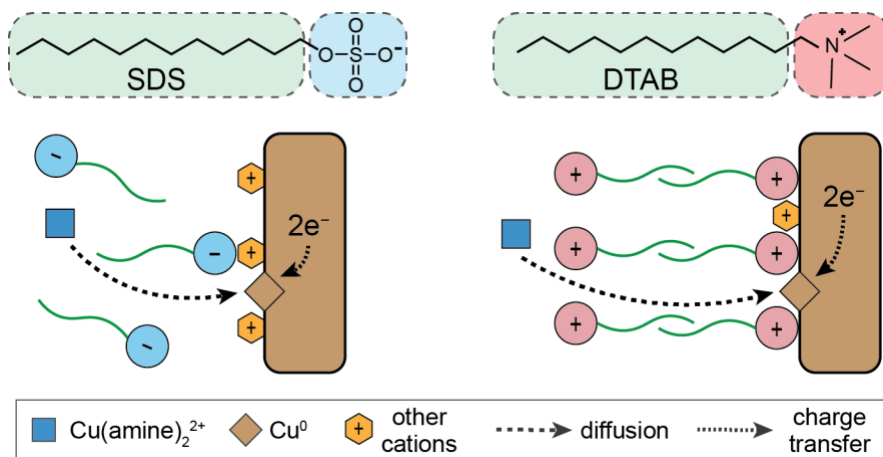


Figure 4. A schematic of the cathode reaction in the presence of SDS (left panel) or DTAB (right panel), in which the charge transfer and diffusion resistances are indicated. The ionic surfactants consist of a hydrophilic head group (blue for SDS and red for DTAB) and a hydrophobic tail (green).

Gas desorption performance. The electrochemical performance of the EMAR system to disengage CO_2 captured from a flue gas stream (15% CO_2 , 85% N_2) was investigated using electrolytes with and without the addition of a surfactant. Various concentrations of SDS as an anionic surfactant, which was shown to have a significantly stronger effect on performance than does the cationic surfactant DTAB, were tested. The concentrations were selected based on the critical micelle concentration (CMC) of SDS calculated in the EMAR electrolyte (data not shown); a value lower than (0.5 mM), equal to (1 mM), or higher than (3 mM) the CMC. Higher concentrations of SDS (5 mM and 13 mM) were also tested, but the results showed high overall resistances, mainly due to the high diffusion resistance (Figure S4). A constant current of 0.5 A was applied to the electrochemical cell, and the desorbed gas flow rate, CO_2 fraction, and cell potential were monitored. Upon application of the electrical current to the cell, CO_2 began to desorb as gas bubbles within the anode compartment. The initial ramping in the desorption profile of all samples shown in Figure 5A indicates approach to anolyte saturation with CO_2 prior to evolution at 1 bar CO_2 , as previously observed in theoretical calculations and experiments.¹⁹ The ramping profiles were not exactly the same in terms of the time required to reach the plateau, likely due to minor differences in the initial gas evolution rate from the electrolyte.¹⁹ The initial ramping was followed by a steady flow of CO_2 for all the studied electrolytes. In terms of the quality of the gas desorbed, the results confirm the purity of the produced CO_2 stream, with no evidence of significant electrolyte evaporation (such as water, amine, or surfactant) (Figure 5A). Overall, the desorption profiles of the

electrolytes containing SDS surfactant were comparable with that of the original EMAR electrolyte.

The key observation during the desorption experiments was the suppression of the formation of copper precipitates in the presence of SDS. In the absence of surfactant, a significant amount of copper precipitate was observed in the stream exiting the anode (as the desorption chamber) (Figure 5B), which accumulated in the flow tubes and flash tank (Figure S5). As mentioned previously, this causes serious damage to the tube and an increase in pressure drop across the flow line. From an operational point of view, this issue may require replacement of the tube and cleaning between cycles, resulting in additional costs. The precipitation issue was effectively avoided in the presence of surfactant; no precipitate was observed in the line or flash tank after running the cell at all SDS concentrations (Figure 5C; Figure S5). This is a key improvement in the EMAR cycle, which would be extremely beneficial for the future development of the process on a large scale.

The elimination of copper precipitate following the addition of SDS surfactant to the electrolyte originates from the controlled stripping of the copper anode offered by the adsorbed layer. Similar to the previous argument regarding the adsorption of DTAB on the negatively charged cathode, SDS as an anionic surfactant forms a bilayer film on the positively charged anode. This layer controls the rate of stripping and likely acts as a protective layer making the electrode resistant to the physical instability caused by the high gas flow rate. This effect has also been observed in previous investigations aimed at inhibition of electrode corrosion by the addition of a surfactant.^{23, 41}

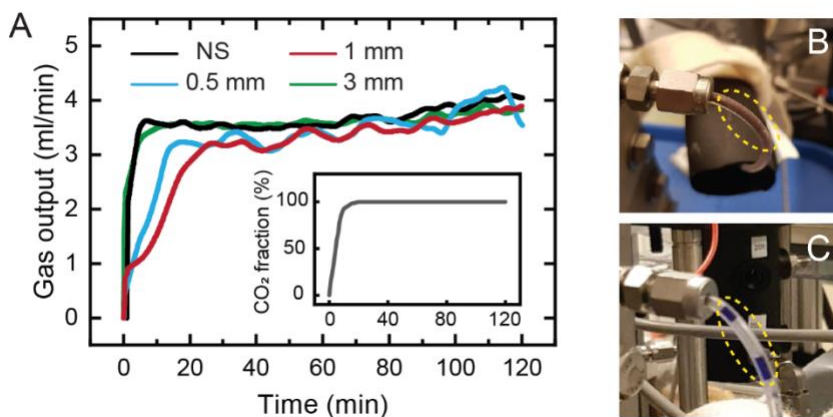


Figure 5. (A) The gas desorption rate and CO₂ fraction (inset panel) of the EMAR process with electrolytes containing no surfactant (NS) or various concentrations of SDS surfactant under constant current (0.5 A) operation. A significant amount of copper precipitate was observed in the flow line exiting the anode after a two-hour experiment without surfactant (panel B), while no precipitate was obtained in the presence of any concentration of SDS even after 6 hours of running the cell (panel C).

Electrochemical energy requirements. To evaluate the desorption performance of EMAR with surfactant in the electrolyte, the electrochemical energy requirement to separate CO₂ from a flue gas was estimated and compared with that in the absence of surfactant. To do so, both the gas flow rate and the cell potentials (obtained under constant current) were considered to estimate the energetics. The cell potential was notably affected by the presence of SDS surfactant as shown in Figure 6; the lowest cell potential was obtained at a surfactant concentration below its CMC, and the potentials increased at higher concentrations. The lowest potential value obtained here (0.4 V for 0.5 mm SDS) is the smallest reported for EMAR to date. The desorption energy requirement followed the same trend as that of the potential with the lowest value in the presence of 0.5 mm SDS, which was ~25% lower than in the absence of surfactant (Figure 6).

The lower potentials obtained in the presence of surfactant can be explained by the impact of this additional compound on the surface tension, which affects the gas bubble size. It has been theoretically and experimentally demonstrated that the use of SDS surfactant reduces the surface tension of a solution (also see Figure S6),^{24, 25} which in the case of EMAR leads to desorption of the gas as smaller bubbles than in the absence of a surfactant. It has previously been shown that the overpotential associated with bubbles attached to an electrode (η_{bubble}) is proportional to the square of the bubble diameter (d),⁴³ i.e., $\eta_{\text{bubble}} \propto d^2$.

Therefore, smaller gas bubbles produced in the presence of the surfactant result in a lowering of η_{bubble} , which is conducive to a reduction in the overall cell potential and the desorption energy requirement of the EMAR process. As the concentration of SDS increased, higher potentials were required to drive the desorption process. The concentrations were intentionally selected to represent values lower than, equal to, and higher than the surfactant CMC. As the surfactant concentration reached the CMC and beyond, a significant increase in the diffusion resistance was observed (Figure S4), mainly because bulky micelles in the diffusion layer are formed, and the adsorbed surfactant layer is more strongly stabilized (Figure 6). This high diffusion resistance for an electrolyte containing the SDS surfactant at a concentration equal to or higher than the CMC offset the favorable impact of the reduction in η_{bubble} due to smaller bubble size. The negatively charged outer layer of the formed micelles can also attract the positively charged electrochemically active species, resulting in a lowering of the local concentrations.

In addition to the impact on bubble size, a reduction in the surface tension facilitates detachment of gas bubbles from the anode, which potentially inhibits pitting and pinholing. This could be an additional reason for the elimination of copper precipitate and physical stability of the electrode, as observed earlier in the presence of SDS surfactant. This further emphasizes the notable role of surfactants in process development.

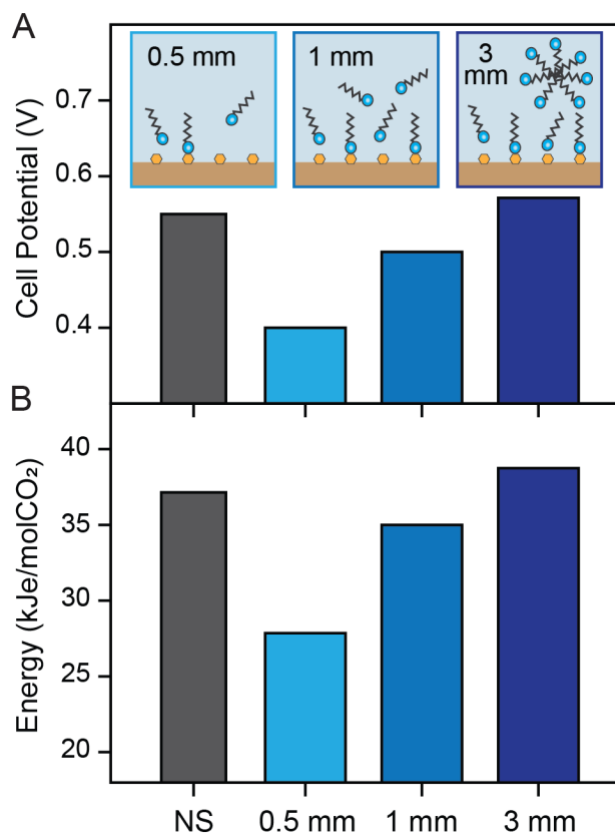


Figure 6. A comparison of (A) cell potential and (B) energy requirement for CO₂ desorption by EMAR with electrolytes containing no surfactant (NS) and various concentrations of SDS. The inset schematics indicate the orientation of the surfactant molecules on the copper cathode electrode and in the solution at different SDS concentrations. The orange symbols represent the counter ions (e.g., Na⁺) adsorbed on the electrode surface.

Conclusions

In the present study, we investigated the effect of the presence of anionic and cationic surfactants in the electrolyte on the EMAR performance. The importance of the surfactant type was highlighted, since for a system such as EMAR with hydrophilic electrodes and a positively charged electrochemically active species, it is essential to use an anionic surfactant in order to improve the electrochemical performance. This enhancement can be attributed to the adsorbed surfactant orientation and its resulting interaction with the electroactive species. The precipitation issue, which could potentially be a serious concern in terms of the operational stability and costs of the EMAR process, was effectively avoided by the use of SDS anionic surfactant, mainly due to the surfactant adsorption configuration on the

electrode, which acted as a protective layer to control the stripping of the copper from the anode. At a concentration of SDS below its CMC, the lowest energetics ever reported experimentally for the EMAR system were achieved. This improvement was mainly associated with the lower cell potential required to drive CO₂ desorption, which originated from the reduction in bubble size (therefore, less electrode blockage by gas) in the presence of surfactant. Overall, the addition of a very low concentration of SDS (on the order of millimolar), as a widely used compound in industry, addressed the issues related to precipitate formation (electrode instability) and further reduced the energy requirement of the process. These are important concerns that needed to be resolved before further scale-up of the system to a pilot scale and beyond can be pursued.

The main focus of this investigation was to study the feasibility and impact of surfactant addition at the process level. In future studies, the impact of surfactant at the microscopic level must be considered to further understand and optimize the process. This may be achieved through the implementation of characterization techniques to carefully monitor the impact of surfactant on the stripping/plating reactions and bubble size during the EMAR cycle. In addition, the rate of surfactant adsorption on the electrode must be carefully investigated to better understand the surface blocking. Common anionic surfactants other than SDS should also be considered. The present study is the first to highlight the substantial impact of anionic surfactants on EMAR performance and provides motivation to exploit expertise developed over decades in the field of surfactants to enhancing carbon capture by EMAR.

Associated Content

Supporting Information

The Supporting Information contains detailed information regarding solution preparation, additional CO₂ loading, CV and EIS measurements, components of ohmic resistance, surface tension results, and a demonstration of the suppression of copper precipitate formed in the anode outlet and flash tank by the added surfactant.

Author Contribution

Conceptualization and Methodology, M.R., and F.Z.; Investigation, F.Z., and M.R.; Writing – Original Draft, M.R.; Writing – Review & Editing, M.R., F.Z., and T.A.H.; Supervision, T.A.H., and M.P.

Notes

The authors declare no competing financial interest.

Acknowledgments

The research was supported by the funding provided by the IHI Corporation in Japan and the Department of Energy under Award Number DE-FE0026489.

References

1. Rogelj, J.; Den Elzen, M.; Höhne, N.; Fransen, T.; Fekete, H.; Winkler, H.; Schaeffer, R.; Sha, F.; Riahi, K.; Meinshausen, M., Paris Agreement climate proposals need a boost to keep warming well below 2 C. *Nature* **2016**, *534*, (7609), 631-639.
2. Luderer, G.; Vrontisi, Z.; Bertram, C.; Edelenbosch, O. Y.; Pietzcker, R. C.; Rogelj, J.; De Boer, H. S.; Drouet, L.; Emmerling, J.; Fricko, O., Residual fossil CO₂ emissions in 1.5–2 C pathways. *Nature Climate Change* **2018**, *8*, (7), 626-633.
3. Rogelj, J.; Huppmann, D.; Krey, V.; Riahi, K.; Clarke, L.; Gidden, M.; Nicholls, Z.; Meinshausen, M., A new scenario logic for the Paris Agreement long-term temperature goal. *Nature* **2019**, *573*, (7774), 357-363.
4. Bui, M.; Adjiman, C. S.; Bardow, A.; Anthony, E. J.; Boston, A.; Brown, S.; Fennell, P. S.; Fuss, S.; Galindo, A.; Hackett, L. A., Carbon capture and storage (CCS): the way forward. *Energy & Environmental Science* **2018**, *11*, (5), 1062-1176.
5. Dutcher, B.; Fan, M.; Russell, A. G., Amine-based CO₂ capture technology development from the beginning of 2013–A Review. *ACS applied materials & interfaces* **2015**, *7*, (4), 2137-2148.
6. Porter, R. T.; Fairweather, M.; Kolster, C.; Mac Dowell, N.; Shah, N.; Woolley, R. M., Cost and performance of some carbon capture technology options for producing different quality CO₂ product streams. *International Journal of Greenhouse Gas Control* **2017**, *57*, 185-195.
7. Scovazzo, P.; Poshusta, J.; DuBois, D.; Koval, C.; Noble, R., Electrochemical separation and concentration of < 1% carbon dioxide from nitrogen. *Journal of The Electrochemical Society* **2003**, *150*, (5), D91-D98.
8. Voskian, S.; Hatton, T. A., Faradaic electro-swing reactive adsorption for CO₂ capture. *Energy & Environmental Science* **2019**, *12*, (12), 3530-3547.

9. Liu, Y.; Ye, H.-Z.; Diederichsen, K. M.; Van Voorhis, T.; Hatton, T. A., Electrochemically mediated carbon dioxide separation with quinone chemistry in salt-concentrated aqueous media. *Nature communications* **2020**, *11*, (1), 1-11.
10. Rahimi, M.; Catalini, G.; Hariharan, S.; Wang, M.; Puccini, M.; Hatton, T. A., Carbon Dioxide Capture Using an Electrochemically Driven Proton Concentration Process. *Cell Reports Physical Science* **2020**, *1*, 100033.
11. Xie, H.; Wu, Y.; Liu, T.; Wang, F.; Chen, B.; Liang, B., Low-energy-consumption electrochemical CO₂ capture driven by biomimetic phenazine derivatives redox medium. *Applied Energy* **2020**, *259*, 114119.
12. Rahimi, M.; Catalini, G.; Puccini, M.; Hatton, T. A., Bench-scale demonstration of CO₂ capture with an electrochemically driven proton concentration process. *RSC Advances* **2020**, *10*, (29), 16832-16843.
13. Liu, C.; Landskron, K., Design, construction, and testing of a supercapacitive swing adsorption module for CO₂ separation. *Chemical Communications* **2017**, *53*, (26), 3661-3664.
14. Legrand, L.; Schaetzle, O.; De Kler, R.; Hamelers, H., Solvent-free CO₂ capture using membrane capacitive deionization. *Environmental science & technology* **2018**, *52*, (16), 9478-9485.
15. Zhu, S.; Li, J.; Toth, A.; Landskron, K., Relationships between the Elemental Composition of Electrolytes and the Supercapacitive Swing Adsorption of CO₂. *ACS Applied Energy Materials* **2019**, *2*, (10), 7449-7456.
16. Khurram, A.; He, M.; Gallant, B. M., Tailoring the Discharge Reaction in Li-CO₂ Batteries through Incorporation of CO₂ Capture Chemistry. *Joule* **2018**, *2*, (12), 2649-2666.
17. Khurram, A.; Yan, L.; Yin, Y.; Zhao, L.; Gallant, B. M., Promoting Amine-Activated Electrochemical CO₂ Conversion with Alkali Salts. *The Journal of Physical Chemistry C* **2019**, *123*, (30), 18222-18231.
18. Stern, M. C.; Simeon, F.; Herzog, H.; Hatton, T. A., Post-combustion carbon dioxide capture using electrochemically mediated amine regeneration. *Energy & Environmental Science* **2013**, *6*, (8), 2505-2517.
19. Wang, M.; Rahimi, M.; Kumar, A.; Hariharan, S.; Choi, W.; Hatton, T. A., Flue gas CO₂ capture via electrochemically mediated amine regeneration: System design and performance. *Applied Energy* **2019**, *255*, 113879.
20. Rahimi, M.; Diederichsen, K. M.; Ozbek, N.; Wang, M.; Choi, W.; Hatton, T. A., An electrochemically mediated amine regeneration process with a mixed absorbent for post-combustion CO₂ capture. *Environmental Science & Technology* **2020**, *54*, (14), 8999-9007.
21. Wang, M.; Herzog, H. J.; Hatton, T. A., CO₂ Capture Using Electrochemically Mediated Amine Regeneration. *Industrial & Engineering Chemistry Research* **2020**, *59*, 7087-7096.
22. Sudagar, J.; Lian, J.; Jiang, Q.; Jiang, Z.; Li, G.; Elansezhan, R., The performance of surfactant on the surface characteristics of electroless nickel coating on magnesium alloy. *Progress in Organic coatings* **2012**, *74*, (4), 788-793.
23. Mousavi, R.; Bahrololoom, M. E.; Deflorian, F., The effect of surfactant on the microstructure and corrosion resistance of electrodeposited Ni-Mo alloy coatings. *Anti-Corrosion Methods and Materials* **2019**.
24. Fernandez, D.; Maurer, P.; Martine, M.; Coey, J.; Mobius, M. E., Bubble formation at a gas-evolving microelectrode. *Langmuir* **2014**, *30*, (43), 13065-13074.
25. Zhao, X.; Ren, H.; Luo, L., Gas bubbles in electrochemical gas evolution reactions. *Langmuir* **2019**, *35*, (16), 5392-5408.
26. Escalona-Durán, F.; Villegas-Guzman, P.; dos Santos, E. V.; da Silva, D. R.; Martínez-Huitle, C. A., Intensification of petroleum elimination in the presence of a surfactant using anodic electrochemical treatment with BDD anode. *Journal of Electroanalytical Chemistry* **2019**, *832*, 453-458.

27. Bastani, D.; Fayzi, P.; Lotfi, M.; Arzideh, S. M., CFD simulation of bubble in flow field: Investigation of dynamic interfacial behaviour in presence of surfactant molecules. *Colloid and Interface Science Communications* **2018**, *27*, 1-10.
28. Rahimi, M.; Kim, T.; Gorski, C. A.; Logan, B. E., A thermally regenerative ammonia battery with carbon-silver electrodes for converting low-grade waste heat to electricity. *Journal of Power Sources* **2018**, *373*, 95-102.
29. Rahimi, M.; Zhu, L.; Kowalski, K. L.; Zhu, X.; Gorski, C. A.; Hickner, M. A.; Logan, B. E., Improved electrical power production of thermally regenerative batteries using a poly (phenylene oxide) based anion exchange membrane. *Journal of Power Sources* **2017**, *342*, 956-963.
30. Wang, M.; Hariharan, S.; Shaw, R. A.; Hatton, T. A., Energetics of electrochemically mediated amine regeneration process for flue gas CO₂ capture. *International Journal of Greenhouse Gas Control* **2019**, *82*, 48-58.
31. Garrett, P. R., Defoaming: Antifoams and mechanical methods. *Current opinion in colloid & interface science* **2015**, *20*, (2), 81-91.
32. Wang, J.; Nguyen, A. V.; Farrokhpay, S., Foamability of sodium dodecyl sulfate solutions: Anomalous effect of dodecanol unexplained by conventional theories. *Colloids and Surfaces A: Physicochemical and Engineering Aspects* **2016**, *495*, 110-117.
33. Rupprecht, H.; Gu, T., Structure of adsorption layers of ionic surfactants at the solid/liquid interface. *Colloid and Polymer Science* **1991**, *269*, (5), 506-522.
34. Atkin, R.; Craig, V. S.; Wanless, E. J.; Biggs, S., Mechanism of cationic surfactant adsorption at the solid-aqueous interface. *Advances in colloid and interface science* **2003**, *103*, (3), 219-304.
35. Tyrode, E.; Rutland, M. W.; Bain, C. D., Adsorption of CTAB on hydrophilic silica studied by linear and nonlinear optical spectroscopy. *Journal of the American Chemical Society* **2008**, *130*, (51), 17434-17445.
36. Harwell, J. H.; Hoskins, J. C.; Schechter, R. S.; Wade, W. H., Pseudophase separation model for surfactant adsorption: isomerically pure surfactants. *Langmuir* **1985**, *1*, (2), 251-262.
37. Schulz, E. N.; Schulz, E. P.; Schulz, P. C., Electrochemistry of Surfactants. *Application and Characterization of Surfactants* **2017**, 261.
38. Li, P.; Ishiguro, M., Adsorption of anionic surfactant (sodium dodecyl sulfate) on silica. *Soil science and plant nutrition* **2016**, *62*, (3), 223-229.
39. Ahualli, S.; Iglesias, G.; Wachter, W.; Dulle, M.; Minami, D.; Glatter, O., Adsorption of anionic and cationic surfactants on anionic colloids: supercharging and destabilization. *Langmuir* **2011**, *27*, (15), 9182-9192.
40. Nevskaiia, D.; Guerrero-Ruiz, A.; López-González, J. d. D., Adsorption of polyoxyethylenic nonionic and anionic surfactants from aqueous solution: Effects induced by the addition of NaCl and CaCl₂. *Journal of colloid and interface science* **1998**, *205*, (1), 97-105.
41. Vittal, R.; Gomathi, H.; Kim, K.-J., Beneficial role of surfactants in electrochemistry and in the modification of electrodes. *Advances in colloid and interface science* **2006**, *119*, (1), 55-68.
42. Tulpar, A.; Ducker, W. A., Surfactant Adsorption at Solid- Aqueous Interfaces Containing Fixed Charges: Experiments Revealing the Role of Surface Charge Density and Surface Charge Regulation. *The Journal of Physical Chemistry B* **2004**, *108*, (5), 1667-1676.
43. Gabrielli, C.; Huet, F.; Keddam, M.; Macias, A.; Sahar, A., Potential drops due to an attached bubble on a gas-evolving electrode. *Journal of applied electrochemistry* **1989**, *19*, (5), 617-629.